



1 Blue Intensity based experiments for reconstructing North 2 Pacific temperatures along the Gulf of Alaska

3
4 Rob Wilson^{1,2}; Rosanne D'Arrigo²; Laia Andreu-Hayles²; Rose Oelkers²; Greg Wiles^{2,3}; Kevin
5 Anchukaitis^{4,2} and Nicole Davi^{2,5}

6 ¹School of Earth and Environmental Sciences, University of Saint Andrews, Saint Andrews, UK;

7 ²Tree-Ring Laboratory, Lamont-Doherty Earth Observatory, Palisades, NY, USA;

8 ³Department of Geology, The College of Wooster, OH, USA;

9 ⁴School of Geography and Development & Laboratory of Tree Ring Research, University of Arizona, Tucson, AZ

10 USA

11 ⁵William Paterson University, New Jersey, USA.

12 *Correspondence to:* Rob Wilson (rjsw@st-andrews.ac.uk)

13

14 **Abstract:** Climate in the Gulf of Alaska (GOA) reflects large-scale ocean-atmosphere variability of the North
15 Pacific climate system. Ring-width (RW) records from the GOA have yielded a valuable long-term perspective for
16 North Pacific changes on decadal to longer time scales in prior studies, but express a broad winter to late summer
17 seasonal response. Similar to the highly climate-sensitive maximum latewood density (MXD) proxy, the Blue
18 Intensity (BI) parameter has recently been shown to correlate well with year-to-year warm-season temperatures for a
19 number of sites at northern latitudes. Since BI records are much less expensive and labor intensive to generate than
20 MXD, such data hold great potential value for future tree-ring studies in the GOA and other regions at mid-to-high
21 latitudes. Here we highlight the potential for improving tree-ring based reconstructions using combinations of RW
22 and BI-related parameters (latewood BI (LWB) and delta BI (DB)) from an experimental sub-set of samples from
23 eight mountain hemlock (*Tsuga mertensiana*) sites along the GOA. This is the first such study for the hemlock
24 genus using BI data. We find that using either LWB or DB can improve the amount of explained temperature
25 variance by > 10% compared to RW alone although the optimal target season changes to June-September, which
26 may have implications for studying ocean-atmosphere variability in the region. However, one challenge in building
27 these BI records is that resin extraction did not remove colour differences between the heartwood and sapwood, so
28 long term trend biases, expressed as relatively warm temperatures in the 18th century, were noted when using the
29 LWB data. Using DB appeared to overcome these trend biases resulting in a reconstruction expressing 18th-19th
30 century temperatures ca. 0.5°C cooler than the 20th/21st centuries. This cool period agrees well with previous
31 dendroclimatic studies and the glacial advance record in the region. Continuing BI measurement in the GOA region
32 must focus on sampling more trees per site (> 20) and more sites to overcome site specific factors effecting climate
33 response while sub-fossil material will extend the reflectance records back over 1000 years. DB appears to capture
34 long term secular trends that agree with other proxy archives in the region but great care is needed when
35 implementing different detrending options. Finally, more experimentation is needed to assess the utility of DB for
36 different conifer species around the Northern Hemisphere.

37
38 **Keywords:** Blue Intensity, Gulf of Alaska, Tree Rings, Reconstruction, North Pacific; **Short Title:** Gulf of Alaska
39 Blue Intensity Tree-Ring Temperature Reconstruction

40

41

42

1. Introduction



43 The climate of the Gulf of Alaska (GOA) is strongly influenced by the atmosphere-ocean variability of the North
44 Pacific sector (e.g. the Pacific Decadal Oscillation, Mantua et al. 1997), with profound socioeconomic implications
45 for the region (Ebbesmeyer et al. 1991). However, the variability of such synoptic climate phenomena is more
46 strongly expressed in winter. Ring-width (RW) data measured from montane treeline conifer trees in the GOA
47 region often express a broad seasonal response window (e.g. January-September, Wilson et al. 2007; February-
48 August, Wiles et al. 2014), which has allowed such data to provide information on cold season synoptic dynamics
49 for almost two thousand years (Barclay et al. 1999, D'Arrigo et al. 2001, Wiles et al. 2004 and 2014, Wilson et al.
50 2007).

51

52 Maximum-latewood density (MXD) measurements have yielded long records of past summer temperatures for many
53 regions in the northern mid-to-high latitudes (e.g. Schweingruber 1988, Briffa et al. 2002, Anchukaitis et al. 2013,
54 Schneider et al. 2015), but such records do not yet exist for the GOA. MXD series are particularly desirable as such
55 records often express stronger coherence with temperatures than RW and result in climate reconstructions with
56 better skill and spectral fidelity (Anchukaitis et al. 2013, Esper et al. 2015, Wilson et al. 2016). This is partly
57 because RW chronologies typically exhibit higher autocorrelation and lagged memory effects than MXD (Briffa et
58 al. 2002; Anchukaitis et al. 2012), but also because RW may potentially integrate other ecological signals (e.g.
59 disturbance and stand dynamics) which can obscure the climate signal (Rydval et al. 2015). Yet, only two
60 millennial-length MXD records are currently published for all of northwestern North America (Icefields, British
61 Columbia (BC), Canada - Luckman and Wilson 2005; Firth River, Alaska - Andreu-Hayles et al. 2011, Anchukaitis
62 et al. 2013) and no traditionally measured MXD data have been generated to date for the entire GOA. This situation
63 partly relates to the expensive and labor intensive nature of MXD measurement, but also because the wood of
64 mountain hemlock (*Tsuga mertensiana*), the dominant conifer species in the GOA, is rather brittle and does not lend
65 itself well to sample preparation for MXD measurement.

66

67 To help meet the need for additional climatically-sensitive density records from northwestern North America, we
68 present herein an exploration of novel Blue Intensity (BI) parameters measured from scanned images of tree core
69 samples from the GOA. Minimum latewood blue intensity (LWB) has recently been shown to express strong
70 similarities to MXD, and is much cheaper and easier to generate (McCarroll et al. 2002; Björklund et al. 2014, 2015;
71 Rydval et al. 2014; Wilson et al. 2014, 2017). LWB is closely related to MXD as they measure similar wood
72 properties (combined hemicellulose, cellulose and lignin content related to cell wall thickness), and both are well
73 correlated with warm-season temperatures (Campbell et al. 2007; Björklund et al. 2014, Rydval et al. 2014, Wilson
74 et al. 2014). This correspondence between BI and temperature has recently been shown to hold true for several
75 locations and tree species, including Scots pine (*Pinus sylvestris*) in Scotland, UK (Rydval et al. 2014) and Sweden
76 (Björklund et al. 2014, 2015), Caucasian fir (*Abies nordmanniana*) in the Northern Caucasus' (Dolgova 2016),
77 Stone pine (*Pinus cembra*) in Austria (Österreicher et al. 2015; Wilson et al. 2017), Engelmann spruce (*Picea
78 engelmannii*) from the Canadian Rockies, British Columbia, Canada (Wilson et al. 2014) and our own analyses of
79 white spruce (*Picea glauca*) in northwestern North America (Andreu-Hayles et al., ms. in prep.). Although BI often



80 requires larger sample sizes than MXD to improve signal strength (Wilson et al. 2014), this is not a concern due to
81 the low cost of the method.

82
83 The greatest limitation of LWB, however, is that any colour variation that does not represent year-to-year climate-
84 driven cell wall thickness changes will bias the resultant raw reflectance measurements. For example, some conifer
85 species (including Scots pine and mountain hemlock) show either a sharp or transitional colour change from the
86 heartwood to sapwood, which, even after resin extraction using ethanol or acetone, can still impose a systematic
87 change in reflectance around the heartwood/sapwood transition (Björklund et al. 2014, 2015). Further colour
88 variations, often seen in dead but preserved snag or sub-fossil wood, can also result in systematic biases when
89 combined with data measured from living samples (Björklund et al. 2014, 2015; Rydval et al. 2014). Björklund et al.
90 (2014) proposed a potential solution to the heartwood/sapwood colour bias issue by effectively detrending the LWB
91 measurements by removing the inherent common colour changes of the earlywood and latewood (i.e. those related
92 to heartwood/sapwood colour change). This was done by subtracting the LWB value from the maximum blue
93 reflectance value of the earlywood (EWB) for each year. The resulting new parameter, referred to as delta blue
94 intensity (hereafter referred to as DB), should theoretically be less biased by such non-climatic related colour
95 changes. Although Björklund et al. (2014, 2015) presented compelling DB results using Scots pine in Sweden, the
96 method has not yet been tested elsewhere or on any other species. We hypothesise that DB can only theoretically
97 work if the inter-annual signal between EWB and LWB is weakly correlated. If the correlation between these two
98 parameters is high, then the method of deriving DB may remove the specific climate signal of interest.

99
100 Finally, although BI based variables hold great promise as an alternative proxy to MXD, another concern is their
101 potential inability to capture low frequency information related to long term-climate changes. Wilson et al. (2014),
102 working with Engelmann spruce from British Columbia, which does not express a visual colour difference, urged
103 caution as both the MXD and LWB parameters were sensitive to different detrending options and there was some
104 indication that LWB could not capture as much low frequency information as MXD. However, this observation
105 could not be fully addressed due to the relatively short instrumental record in British Columbia.

106
107 In this paper, building upon previous RW based research (Wilson et al. 2007, Wiles et al. 2014), we measure BI
108 variables (EWB, LWB and DB) from multiple sites in the GOA to evaluate: (a) whether BI can improve on previous
109 RW-only based reconstruction, and (b) whether meaningful low frequency information can be gleaned from these
110 data by exploiting the long monthly instrumental temperature records that go back into the mid-19th century to
111 validate secular trends in the TR data.

112

113

114

115

116 **2. Methods and Analysis**



117

118 BI measurements were made on a sub-set (ca. 15 single tree cores per site) of crossdated core samples collected over
119 the past few decades from living mountain hemlock (*Tsuga mertensiana* Bong. Carrière) trees located at eight sites
120 near altitudinal treeline (around ~300-400 meters above sea level) along the GOA (Table 1, Figure 1). Data from
121 these and additional sites were used previously to create coastal GOA RW based temperature-related reconstructions
122 (D'Arrigo et al. 2001, Wilson et al. 2007, Wiles et al. 2014).

123

124 The tree core samples were immersed in acetone for 72 hours to remove excess resins in the wood (Rydval et al.
125 2014) and then finely sanded to 1200 grit to remove marks and abrasions prior to scanning. An Epson V850 pro
126 scanner, using an IT-8 calibration card in conjunction with Silverfast scanning software, was used to scan the
127 samples at 2400 dpi resolution. EWB and LWB variables were measured using the CooRecorder 8.1 software
128 (Cybis 2016 - <http://www.cybis.se/forfun/dendro/index.htm>), which has state-of-the-art capabilities to acquire
129 accurate reflectance intensity RGB colour measurements from scanned wood samples (see Rydval et al. 2014). DB
130 values were calculated within CooRecorder by subtracting the LWB values from the EWB values for each year.
131 Since LWB is negatively correlated to MXD (high density 'dark' latewood = low reflectance), values were inverted
132 following the method detailed in Rydval et al. (2014) to allow for LWB to be detrended in a similar way to MXD
133 (see also Wilson et al. 2014). The nature of the DB calculation results in this parameter being positively correlated
134 with inverted LWB, so these data could also be theoretically detrended in a similar way.

135

136 For initial experiments comparing the different tree-ring (TR) variables, the RW, LWB, EWB and DB data were
137 detrended using fixed 200-year cubic smoothing splines (Cook and Peter 1981) to retain the interannual to decadal
138 signal and minimize any potential lower frequency biases due to heartwood/sapwood colour changes. These
139 chronology versions were assessed by (1) signal strength statistics: both common signal (via mean inter-series
140 correlation – R_{BAR}) and expressed population signal (EPS - Wigley et al. 1984) statistics, (2) between variable
141 correlation, (3) between site coherence using a rotated principal component analysis (PCA, varimax rotation using
142 correlation matrices with eigenvectors retained with an eigenvalue > 1.0) and (4) climate response derived by
143 correlations between regional composite TR variable mean series and the dominant PC scores against monthly and
144 season variables of temperature (CRU TS 3.24 (Harris et al. 2012): 57-61°N / 153-134°W).

145

146 The 200-year spline chronology versions were also used to explore calibration (1901-1960) and validation (1961-
147 1989) based principal component regression reconstruction experiments using the CRU TS data. For the PCA, a
148 reasonably replicated common period (1792-1989) was used where tree series replication was > 5 trees. All site
149 chronologies are replicated with > 10 trees from 1792 except for JM and SR (see Table 1) where replication is 6 and
150 5, respectively. Reconstruction validation was performed using the Pearson's correlation coefficient (r), the
151 Reduction of Error (RE) and the Coefficient of Efficiency (CE - Cook et al., 1994). Further validation was
152 performed over the 1850-1900 period using the gridded BEST instrumental data (Rohde et al., 2012), extracted for
153 the same region as the CRU TS (57-61°N / 153-134°W), after these data were scaled to the CRU TS data over the



154 1901-2015 period. CRU TS and BEST compare well to the original GOA 5-station mean record (Supplementary
155 Figure 1) used in Wilson et al. (2007) confirming that the gridded products are good representations of the regional
156 temperature signal. The higher variance of the pre-1950 period in the 5-station mean is related to the fact that
157 variance stabilization (Frank et al. 2007a) was not performed when this mean series was originally developed
158 (Wilson et al. 2007) and is therefore likely a less robust measure of GOA temperatures than the gridded products.
159

160 Finally, to explore the potential of reconstructing robust low frequency temperature changes in the region, the data
161 from each of the eight sites were pooled to derive GOA regional composite records for each of the TR variables.
162 These pooled composite variable datasets, with their greater overall replication, allowed detrending experiments to
163 be performed to ascertain the sensitivity of the final parameter chronologies to different detrending choices.
164 Specifically, RW detrending experiments were performed using (1) STD: negative exponential function or negative
165 or zero slope linear function detrending via division; (2) NEPT: negative exponential function or negative or zero
166 slope linear function detrending via subtraction after power transformation of the raw RW data (Cook and Peters
167 1997); (3) RCS: single group regional curve standardization (RCS - Briffa et al., 1996; Esper et al., 2003; Briffa and
168 Melvin 2008) detrending via division. For each of these three approaches, the 'Signal-Free' (SF - Melvin and Briffa
169 2008) approach to detrending was also utilized. These different options resulted in 6 different RW composite
170 chronologies. For LWB and DB, as they theoretically should behave more like MXD, detrending was performed
171 using only two methods; (1) LINres: negative or zero slope linear function detrending via subtraction; (2) RCSres:
172 single group RCS detrending via subtraction. As with the RW data, the SF approach was also performed leading to
173 four chronology variants for both LWB and DB.
174

175 **3. Results and Discussion**

176 **3.1 Common signal within the network**

177 RW has the strongest common signal with a median overall RBAR of 0.44 (8 site range: 0.33 – 0.49 - Table 1),
178 whereas LWB and DB both have weaker RBAR values of 0.24. EWB shows the weakest common signal with a
179 median RBAR from the 8 sites of only 0.12. In order of decreasing between-series common signal, the number of
180 series needed to attain an EPS of 0.85 are 7 (RW), 18 (LWB and DB), and 41 (EWB) for each TR variable
181 respectively. Rydval et al. (2014) showed that as the within tree common signal was much weaker for LWB than
182 RW, the between tree common signal improved more for LWB than RW as multiple radii from the same tree were
183 measured (i.e. up to 3). For this exploratory analysis, only a single series was measured per tree, and therefore we
184 hypothesise that the EPS of BI based chronologies would improve markedly, compared to RW, if at least 2 radii
185 were measured from each tree.
186

187 The weak signal strength in EWB compared to RW, LWB and DB is also reflected in the PCA. The leading PC for
188 RW, LWB and DB explains 59%, 53% and 57% of the overall variance, respectively, while just 39% is explained by
189 the EWB PC1. In general, the loadings (based on a varimax rotation) of the chronologies on each PC for each



190 variable are related to the geographical locations across the GOA with PC1 representing the eastern sites and PC2
191 the western ones (Figures 1 and 2).

192

193 **3.2 Seasonal temperature sensitivity**

194 EWB contains a weak response to summer temperature variability with almost no late summer temperature signal
195 (Figure 2) although significant correlations ($r = \sim 0.3 - 0.4$) are found with May and previous October/November
196 temperatures (supplementary Figure 2). In agreement with previous work (Wilson et al. 2007; Wiles et al. 2014),
197 RW correlates well with a broad range of summer seasons, showing positive correlations for nearly all months from
198 January through to September (Supplementary Figure 2) with June returning the strongest correlation. LWB and
199 DB, on the other hand, show weaker responses with the late winter/spring months and strongest correlations with
200 June, July and August (Figure 2). As LWB and DB should express similar growth/climate response properties to
201 MXD, these observations are not surprising.

202

203 There appears to be a geographical difference in response with PC1 (eastern sites) showing stronger seasonal
204 (Figure 2) and monthly (supplementary Figure 2) correlations with temperature than PC2 (western sites). This
205 spatial pattern of response is also expressed in the RW data (Figure 2). However, correlations of the individual site
206 chronologies for each TR variable (Table 2) against June-September temperatures (optimal season for reconstruction
207 – see later) suggest that there is a degree of variability of the individual sites' response to summer temperatures
208 across the GOA. As PC2 is weighted more towards the TBB site (see PCA loadings in Figure 2 for RW, LWB and
209 DB) which correlates weakly with JJAS, it is therefore not surprising that this PC correlates weakly with summer
210 temperatures. However, the correlation results of the mean composite chronologies (Figure 2) are marginally
211 stronger than the PC1 results. This suggests that a regional mean composite approach is potentially optimal in the
212 context of deriving a GOA wide reconstruction which can be extended further back in time using data generated
213 from sub-fossil samples.

214

215 The positive correlation of RW, LWB and DB to summer temperatures (Figure 2 and Table 2) is also reflected in the
216 inter-correlation between these different variables (Table 3). RW agrees most strongly with DB, followed by LWB.
217 EWB has the weakest relationship with the other 3 variables. Importantly, the correlation between EWB and LWB is
218 weak which we hypothesise is the theoretical ideal for the utilization DB to minimize potential heartwood/sapwood
219 colour change biases (Björklund et al. 2014, 2015). Hereafter, due to the poor signal strength and weak climate
220 signal, the EWB data alone was not used for further analysis except in the DB calculations.

221

222 **3.3 Calibration/validation experiments**

223 Calibration and validation statistics for various PC regression variable combinations for several summer target
224 seasons are detailed in Table 4 along with results using the GOA RW composite of Wiles et al. (2014). Firstly,
225 calibration of Wiles et al. (2014) to the CRU TS 3.24 data (February – August) over the 1901-1989 period ($r^2 =$
226 0.33) is stronger than the new sample sub-set based RW GOA composite ($r^2 = 0.27$) which also shows a significant



227 trend in the model residuals. This residual trend possibly reflects the fact that there could be a longer term low
228 frequency trend missing in the RW data due to the use of 200-year spline detrended chronologies when compared to
229 the RCS processed version of Wiles et al. (2014). Also, the slightly weaker results of the new RW data likely reflect
230 generally lower replication in the current study compared to Wiles et al. (2014).

231

232 The strongest calibration a_r^2 values for each BI parameter over the 1901-1960 period are 0.49 and 0.47 for LWB and
233 DB respectively for the JJA season although DB fails validation with negative RE and CE values over the 1961-
234 1989 period. Minimal model improvement is gained by including RW data. RW+LWB calibrates best ($a_r^2 = 0.49$)
235 with JJA while RW+DB explains more temperature variance for MJJAS ($a_r^2 = 0.51$). However, in both cases,
236 validation RE and CE are negative. Focussing on the full period (1901-1989) calibration, strongest results are found
237 for the JJAS season for all parameters options (except Feb-Aug for RW) with a_r^2 values of 0.27 (RW), 0.43 (LWB),
238 0.38 (DB), 0.38 (RW+LWB) and 0.39 (RW+DB) with no 1st order autocorrelation noted for any version. Only the
239 RW+DB version, however, shows no significant linear trend in the model residuals. The full period (1901-1989)
240 calibrated reconstructions (Table 4) for each of the variable options are presented in Figure 3 along with independent
241 validation (1850-1900) with the BEST gridded data. All parameter iterations fail validation (negative CE values)
242 except for RW+DB which returns positive RE (0.57) and CE (0.19) values. Overall, using this subset of samples
243 from these 8 sites, the calibration results (Table 4 and Figure 3) indicate that BI based parameters explain more
244 temperature variance than using RW alone. However, assessing the fidelity of the resultant reconstructions appears
245 sensitive to the periods of calibration and validation used and as the chronologies were limited in the frequency
246 domain by using a fixed 200-year spline detrending option, it is not clear which of these parameters best represent
247 longer term secular change.

248

249 The large-scale climate signal expressed by these data is illustrated by comparing the RW+DB JJAS reconstruction
250 with gridded land/sea HadCRUT4 (Morice et al. 2012; Cowtan and Way 2014 – Figure 4a) and land only CRU TS
251 3.24 (Harris et al. 2012 – Figure 4b) temperatures for the GOA and North Pacific sector. Although the spatial
252 correlations are stronger towards Juneau and Sitka (see Figure 1 for locations) in the east of the region it is clear that
253 these new data represent very well the temperature variability of the wider GOA region and North Pacific.
254 Continued measurement of BI based parameters from sub-fossil samples taken from each end of the GOA will allow
255 long term summer temperature variability to be derived for at least the last millennium which will complement the
256 long RW based temperature reconstructions expressing a broader seasonal window (Wilson et al. 2007; Wiles et al.
257 2014).

258

259 3.4 Potential low frequency bias

260 The main potential limitation to the use of BI based TR variables such as LWB is concerned with low frequency
261 trend biases related to wood colour change. Mountain hemlock, in general, shows darker heartwood and lighter
262 sapwood, a colour change which resin extraction appears to only minimise but not entirely remove. Also, this colour
263 change is not a sharp transition and is expressed in raw EWB and LWB measurements as a steady increase in



264 reflectance intensity. Non-detrended mean composite chronologies of EWB and LWB for the whole GOA region
265 (Figure 5) clearly show the impact of the heartwood/sapwood colour change with increasing intensity values through
266 time (see also Supplementary Figure S3 for a single tree example), especially since the late 18th century. However,
267 MXD generally shows a linear decreasing trend with increasing cambial age (Esper et al. 2012). If LWB is indeed a
268 comparable (but inverted) TR variable to MXD as a measure of latewood anatomical density properties, then we
269 would expect, therefore, an increasing trend in raw LWB values. Figure 5 therefore poses a potential “mixed-signal”
270 conundrum as the observed trend in the GOA raw mean LWB composite will incorporate both the true age-related
271 trend of changing latewood density and the heartwood/sapwood colour change bias. Although using DB can
272 theoretically overcome these colour bias issues, it has not been explored in any detail beyond the original concept
273 papers (Björklund et al. 2014, 2015). The mean DB non-detrended GOA chronology (Figure 5) expresses minimal
274 long term trends which could suggest that the colour change bias has been removed or at least minimised.

275

276 Mean cambial age-aligned curves of the LWB and DB data show very distinct trends (Supplementary Figure 4).
277 LWB appears to show a general linear increase in values – a trend that would be expected if LWB indeed does
278 reflect similar wood properties (inversely) to MXD. DB, however, has a more complex mean growth curve and
279 shows an initial increasing juvenile trend for ~50 years, a period of stabilisation and then a decreasing trend from
280 about ~200 to 300 years. These different age-aligned curves highlight that different detrending options may well be
281 needed for these different TR variables.

282

283 A range of credible methodological choice options for detrending the RW, LWB and DB GOA regional composite
284 data are presented in Figure 6. The outcome for the RW data appears extremely consistent even when using STD vs
285 RCS based methods. However, the LWB and DB chronologies are extremely sensitive to the detrending method
286 used. Compared to RW and DB, all LWB chronology variants show above zero z-score values in the 17th century,
287 which likely reflects the low reflectance bias of the darker heartwood compared to the sapwood because the LWB
288 data have been inverted. The RCS versions appear particularly inflated and as LWB is positively correlated with
289 summer temperatures (Figure 2), this would result in markedly warm temperature estimates during the LIA
290 compared to the 20th century which is at odds with previous GOA dendroclimatic analyses (Wiles et al. 2014) and
291 the geomorphological record, which indicates substantial glacial advance from the 17th to 19th centuries (Wiles et al.,
292 2004; Solomina et al. 2016). RCS can impart significant low frequency bias when the assumptions and requirements
293 of the method are not met (Melvin and Briffa 2014; Anchukaitis et al. 2013) and as the GOA composite utilises only
294 living trees this is a far from optimal sample design for this detrending method. For DB, the LINsf version deviates
295 markedly from LINres, RCSres and RCSsf variants with very low values (< -6 standard deviation from 1901-1989
296 mean) before 1700 followed by a strong linear increase until present. A similar observation was noted in Wilson et
297 al. (2014) where signal free detrending of LWB and especially MXD resulted in much cooler LIA conditions than
298 other detrending approaches.

299

300



301 3.5 JJAS GOA summer temperatures back to 1600

302 The long GOA instrumental record allows for additional assessment of how different reflectance based chronology
303 variants track temperatures back through time. Using the extended BI based regional composite records, further
304 reconstruction experiments against the JJAS season were performed using LWB and DB separately by calibrating
305 against JJAS CRU TS3.24 (1901-2010) and separately validating using the BEST data (1850-1900). For the LWB
306 data, RCSres and RCSsf calibrated poorly (Table 5: $r^2 = 0.07$ and 0.05 respectively) with negative CE values over
307 the 1850-1900 period. The LINres and LINsf version, however, explained 41% of the temperature variance and
308 validated reasonably well with positive RE and CE values. Significant 1st-order autocorrelation (DW range 1.28 to
309 1.37) and linear trends (LINr range 0.36 to 0.48) was however noted for all model residuals. The DB chronology
310 variants on the whole performed better than their LWB counterparts, with RCSsf (RCSres) calibrating most strongly
311 ($r^2 = 0.43$ (0.40)) and validating well (RE = 0.48 (0.50), CE = 0.15 (0.18)). The residuals for both versions show no
312 1st-order autocorrelation although a significant linear trend is still however observed.

313

314 The best reconstructions using LWB (LINres) and DB (RCSsf), identified using the calibration and verification
315 results (Table 5), represent quite different histories of past GOA temperatures (Figure 7). Specifically, the LWB
316 (LINres) reconstruction expresses temperature estimates from the late 17th to mid-19th century warmer than the
317 1961-1990 mean, while the DB (RCSsf) reconstruction exhibits generally cooler conditions. Both reconstructions
318 explain a similar amount of summer temperature variance and validate well (Table 5) and from comparison to the
319 instrumental data alone, one cannot objectively choose which of the two is most robust although there are arguably
320 less problems with the model residuals using the DB data. Wilson et al. (2014) highlighted the difficulties of relying
321 solely on the instrumental data to validate the long-term trend in any reconstruction. Moreover, there could be
322 unknown homogeneity issues in early instrumental data series which are difficult to identify which would impact
323 calibration and validation (see Frank et al. 2007b). Therefore, alternative sources of relevant information are needed
324 for further validation. As the geomorphological record in the region suggests a prolonged period of glacial advance
325 occurred in the GOA up to the early 20th century (Wiles et al., 2004; Solomina et al. 2016) when a substantial retreat
326 started, we hypothesize that the pre-1900 period must therefore have been cooler. This would suggest that the DB
327 based reconstruction is likely more representative of past GOA temperatures than the LWB driven one.

328

329 Figure 8 presents the RW + DB principal component reconstruction (Figure 3), the DB (RCSsf) extended
330 reconstruction (Figure 6) and the Wiles et al. (2014) RW based reconstruction and compares them to the GOA
331 regional glacial advance record (Wiles et al., 2004; Solomina et al. 2016). The TR reconstructions demonstrate
332 centennial and multi-decadal agreement, although the extended DB reconstruction has a smaller amplitude of
333 temperature change between the LIA period and the 20th century. Overall, temperatures in the GOA region were
334 below the 1961-90 norm throughout most of the LIA with temperatures only rising to substantially higher values in
335 the early 20th century. The coldest decadal periods are centred around the 1700s, 1750s, and 1810s. The glacial
336 advance record clearly shows periods of advance through the LIA, peaking at the end of the 19th century. Despite the
337 use of 200-year spline detrended chronologies, the RW+DB reconstruction has a similar amplitude change to the



338 Wiles et al. (2014) record, which was derived from RCS processed RW data. It should however be noted also that
339 this RW based reconstruction was calibrated against Feb-August temperatures which has a greater increasing
340 temperature trend ($0.81^{\circ}\text{C}/\text{century}$ vs $0.62^{\circ}\text{C}/\text{century}$) and higher variance (0.79 vs 0.41) than JJAS (calculated using
341 BEST data from 1850-2015), which will influence the amplitude of the reconstructions (Esper et al. 2005).

342

343 4. Conclusions

344 We have described a set of experimental temperature reconstructions based on RW, LWB and DB data measured
345 from eight tree-ring sites along the Gulf of Alaska. Focusing on these data sets, the results demonstrate that
346 inclusion of BI based variables can significantly improve the calibrated variance explained using RW alone by more
347 than 10%.

348

349 RW, LWB and DB are strongly correlated with each other (Table 3) but the inclusion of LWB or DB shifts the
350 calibrated signal from a broad (February-August, Wiles et al. 2014) season using RW alone to a late summer (JJAS)
351 season. The influence of late winter and early spring temperatures on RW suggest that this variable may, in fact, still
352 be the more optimal variable for studying important synoptic phenomena such as north Pacific variability, which
353 dominates in the winter/spring months (Wilson et al. 2007).

354

355 The LWB data, for mountain hemlock, despite calibrating and validating in a similar way to DB, are clearly affected
356 by heartwood/sapwood colour differences which impart a trend bias in the resultant chronologies and
357 reconstructions (Figure 6 and 7). However, this bias may not necessarily always occur for other species showing a
358 heartwood/sapwood colour change which could be removed through traditional resin extraction methods. For the
359 first time since the original concept papers by Björklund et al. (2014, 2015), we have experimented with the DB
360 variable and the resulting reconstruction agrees well with a previous RW based reconstruction (Wiles et al. 2014)
361 and the glacial advance record (Wiles et al., 2004; Solomina et al. 2016) for the region.

362

363 The analyses presented herein must be viewed as a series of experiments to inform future dendroclimatologists of
364 possible methodological strategies that need to be considered for improving TR based reconstructions using blue
365 reflectance based variables. Specific to the GOA region, but likely relevant to other regions and species, we
366 therefore detail the following recommendations:

367

- Although MXD typically has a higher expressed signal strength and climate responses than RW (Wilson and Luckman 2003), signal strength in LWB and DB in GOA hemlock is weaker than RW, so replication needs to be substantially increased (ideally > 20 trees – Table 1) to allow the development of robust chronologies. Rydval et al. (2014) also showed that substantial improvement in LWB signal strength could be gained by measuring 2 or even 3 radii per tree. Additional assessments of signal strength should be conducted as new species and sites are analysed using BI methods.

371

- For conifer species with a clear colour difference between the heartwood and sapwood, LWB may likely always express biased long-term trends. The DB variable could potentially minimize this effect as shown

374



375 here, but more experimentation with this parameter is needed before it can be commonly used as a solution
376 to the LWB colour bias problem. Rydval et al. (2017) overcame the heartwood/sapwood colour bias by
377 utilising a band-pass approach to calibration, where LWB drove the decadal and high frequency fraction of
378 the Scottish temperature reconstruction, while RW drove the low frequency variability. This approach
379 however assumes that (1) RW is predominantly controlled by summer temperatures (not necessarily the
380 case in the GOA) and (2) meaningful longer-term secular information can be gleaned from RW data, which
381 may not always be the case (Esper et al. 2012).

382 • The results presented herein highlighted substantial sensitivity of the final chronologies to varying
383 methodological detrending approaches. Much more exploration of the impact of different detrending
384 choices is needed for dendroclimatology as a whole. Locations with long instrumental records may help
385 identify more optimal detrending options but care is needed, as it cannot be assumed that the quality of 19th
386 century data is comparable to late 20th/early 21st century data. Utilizing other proxy observations of past
387 climate (e.g. in this case the glacial record) may help further constrain TR estimates of past climate
388 especially when different chronology variants (that validate well) portray quite different past temperature
389 histories.

390
391 **Acknowledgments.** This is a contribution to the PAGES 2k Network [through the Arctic/North America-2k
392 working groups]. Past Global Changes (PAGES) is supported by the US and Swiss National Science Foundations.
393 We also gratefully acknowledge the National Science Foundation's Paleoclimatic Perspectives on Climatic Change
394 (P2C2) Grant Nos. AGS 1159430, AGS 1502186 and AGS1502150. Lamont-Doherty Earth Observatory
395 Contribution No. 0000.

396

397 5. References

398 Anchukaitis, K.J., Breitenmoser, P., Briffa, K.R., Buchwal, A., Büntgen, U., Cook, E.R., D'arrigo, R.D., Esper, J.,
399 Evans, M.N., Frank, D. and Grudd, H., 2012. Tree rings and volcanic cooling. *Nature Geoscience*, 5(12), pp.836-
400 837.

401

402 Anchukaitis, K.J., D'Arrigo, R.D., Andreu-Hayles, L., Frank, D., Verstege, A., Curtis, A., Buckley, B.M., Jacoby,
403 G.C. and Cook, E.R., 2013. Tree-ring-reconstructed summer temperatures from northwestern North America during
404 the last nine centuries. *Journal of Climate*, 26(10), pp.3001-3012.

405

406 Andreu-Hayles, L., D'Arrigo, R., Anchukaitis, K.J., Beck, P.S., Frank, D. and Goetz, S., 2011. Varying boreal forest
407 response to Arctic environmental change at the Firth River, Alaska. *Environmental Research Letters*, 6(4),
408 p.045503.

409

410 Barclay, D.J., Wiles, G.C. and Calkin, P.E., 1999. A 1119-year tree-ring-width chronology from western Prince
411 William Sound, southern Alaska. *The Holocene*, 9(1), pp.79-84.



- 412
- 413 Björklund, J.A., Gunnarson, B.E., Seftigen, K. and Esper, J., 2014. Blue intensity and density from northern
414 Fennoscandian tree rings, exploring the potential to improve summer temperature reconstructions with earlywood
415 information. *Climate of the Past*, 10(2), p.877.
- 416
- 417 Björklund, J., Gunnarson, B.E., Seftigen, K., Zhang, P. and Linderholm, H.W., 2015. Using adjusted Blue Intensity
418 data to attain high-quality summer temperature information: A case study from Central Scandinavia. *The Holocene*,
419 25(3), pp.547-556.
- 420
- 421 Briffa, K.R., Jones, P.D., Schweingruber, F.H., Karlén, W. and Shiyatov, S.G., 1996. Tree-ring variables as proxy-
422 climate indicators: problems with low-frequency signals. In *Climatic variations and forcing mechanisms of the last*
423 *2000 years* (pp. 9-41). Springer Berlin Heidelberg.
- 424
- 425 Briffa, K.R., Osborn, T.J., Schweingruber, F.H., Jones, P.D., Shiyatov, S.G. and Vaganov, E.A., 2002. Tree-ring
426 width and density data around the Northern Hemisphere: Part 1, local and regional climate signals. *The Holocene*,
427 12(6), pp.737-757.
- 428 Briffa, K.R. and Melvin, T.M., 2011. A closer look at regional curve standardization of tree-ring records:
429 justification of the need, a warning of some pitfalls, and suggested improvements in its application. In
430 *Dendroclimatology* (pp. 113-145). Springer Netherlands.
- 431
- 432 Campbell, R., McCarroll, D., Loader, N.J., Grudd, H., Robertson, I. and Jalkanen, R., 2007. Blue intensity in *Pinus*
433 *sylvestris* tree-rings: developing a new palaeoclimate proxy. *The Holocene*, 17(6), p.821.
- 434
- 435 Cook, E.R. and Peters, K., 1997. Calculating unbiased tree-ring indices for the study of climatic and environmental
436 change. *The Holocene*, 7(3), pp.361-370.
- 437
- 438 Cowtan, K. and Way, R.G., 2014. Coverage bias in the HadCRUT4 temperature series and its impact on recent
439 temperature trends. *Quarterly Journal of the Royal Meteorological Society*, 140(683), pp.1935-1944.
- 440
- 441 D'Arrigo, R., Villalba, R. and Wiles, G., 2001. Tree-ring estimates of Pacific decadal climate variability. *Climate*
442 *Dynamics*, 18(3-4), pp.219-224.
- 443
- 444 Dolgova, E., 2016. June–September temperature reconstruction in the Northern Caucasus based on blue intensity
445 data. *Dendrochronologia*, 39, pp.17-23.
- 446
- 447 Ebbesmeyer, C.C., D.R. Cayan, D.R. McLain, F.H. Nichols, D.H. Peterson and K.T. Redmond, 1991:1976 step in
448 the Pacific climate: Forty environmental changes between 1968-75 and 1977-1984. In: *Proc. 7th Ann. Pacific*



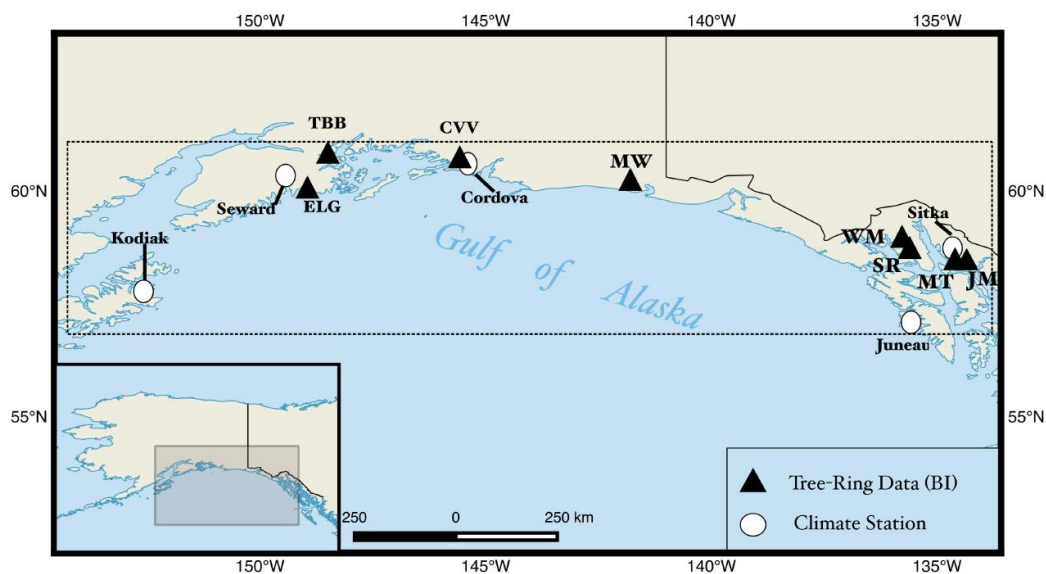
- 449 Climate Workshop, Calif. Dept. of Water Resources, Interagency Ecol. Stud. Prog. Report 26.
450
- 451 Esper, J., Cook, E.R., Peters, K. and Schweingruber, F.H., 2003. Detecting low frequency tree-ring trends by the
452 RCS method. *Tree-Ring Research*, 59(2), pp.81-98.
453
- 454 Esper, J., Frank, D.C., Wilson, R.J. and Briffa, K.R., 2005. Effect of scaling and regression on reconstructed
455 temperature amplitude for the past millennium. *Geophysical Research Letters*, 32(7).
456
- 457 Esper, J., Frank, D.C., Timonen, M., Zorita, E., Wilson, R.J., Luterbacher, J., Holzkämper, S., Fischer, N., Wagner,
458 S., Nievergelt, D. and Verstege, A., 2012. Orbital forcing of tree-ring data. *Nature Climate Change*, 2(12), pp.862-
459 866.
460
- 461 Esper, J., Schneider, L., Smerdon, J.E., Schöne, B.R. and Büntgen, U., 2015. Signals and memory in tree-ring width
462 and density data. *Dendrochronologia*, 35, pp.62-70.
463
- 464 Frank, D., Esper, J. and Cook, E.R., 2007a. Adjustment for proxy number and coherence in a large-scale
465 temperature reconstruction. *Geophysical Research Letters*, 34(16).
466
- 467 Frank, D., Büntgen, U., Böhm, R., Maugeri, M. and Esper, J., 2007. Warmer early instrumental measurements
468 versus colder reconstructed temperatures: shooting at a moving target. *Quaternary Science Reviews*, 26(25),
469 pp.3298-3310.
470
- 471 Harris, I.P.D.J., Jones, P.D., Osborn, T.J. and Lister, D.H., 2014. Updated high-resolution grids of monthly climatic
472 observations—the CRU TS3. 10 Dataset. *International Journal of Climatology*, 34(3), pp.623-642.
473
- 474 Luckman, B.H. and Wilson, R.J.S., 2005. Summer temperatures in the Canadian Rockies during the last millennium:
475 a revised record. *Climate Dynamics*, 24(2-3), pp.131-144.
476
- 477 Mantua, N.J., Hare, S.R., Zhang, Y., Wallace, J.M. and Francis, R.C., 1997. A Pacific interdecadal climate
478 oscillation with impacts on salmon production. *Bulletin of the American Meteorological Society*, 78(6), pp.1069-
479 1079.
480
- 481 McCarroll, D., Pettigrew, E., Luckman, A., Guibal, F. and Edouard, J.L., 2002. Blue reflectance provides a
482 surrogate for latewood density of high-latitude pine tree rings. *Arctic, Antarctic, and Alpine Research*, pp.450-453.
483
- 484 Melvin, T.M. and Briffa, K.R., 2008. A “signal-free” approach to dendroclimatic standardisation.
485 *Dendrochronologia*, 26(2), pp.71-86.



- 486
487 Melvin, T.M. and Briffa, K.R., 2014. CRUST: Software for the implementation of Regional Chronology
488 Standardisation: Part 2. Further RCS options and recommendations. *Dendrochronologia*, 32(4), pp.343-356.
489
490 Morice, C.P., Kennedy, J.J., Rayner, N.A. and Jones, P.D., 2012. Quantifying uncertainties in global and regional
491 temperature change using an ensemble of observational estimates: The HadCRUT4 data set. *Journal of Geophysical*
492 *Research: Atmospheres*, 117(D8).
493
494 Österreicher, A., Weber, G., Leuenberger, M. and Nicolussi, K., 2015. Exploring blue intensity-comparison of blue
495 intensity and MXD data from Alpine spruce trees. *TRACE–Tree Rings in Archaeology, Climatology and Ecology*,
496 13, pp.56-61.
497
498 Rohde, R., Muller, R.A., Jacobsen, R., Muller, E., Perlmutter, S., Rosenfeld, A., Wurtele, J., Groom, D. and
499 Wickham, C., 2012. A new estimate of the average Earth surface land temperature spanning 1753 to 2011. *Geoinfor*
500 *Geostat: An Overview*, 1(1), pp.1-7.
501
502 Rydval, M., Larsson, L.Å., McGlynn, L., Gunnarson, B.E., Loader, N.J., Young, G.H. and Wilson, R., 2014. Blue
503 intensity for dendroclimatology: should we have the blues? Experiments from Scotland. *Dendrochronologia*, 32(3),
504 pp.191-204.
505
506 Rydval, M., Druckenbrod, D., Anchukaitis, K.J. and Wilson, R., 2015. Detection and removal of disturbance trends
507 in tree-ring series for dendroclimatology. *Canadian Journal of Forest Research*, 46(3), pp.387-401.
508
509 Rydval, M., Loader, N.J., Gunnarson, B.E., Druckenbrod, D.L., Linderholm, H.W., Moreton, S.G., Wood, C.V. and
510 Wilson, R., 2017. Reconstructing 800 years of summer temperatures in Scotland from tree rings. *Climate Dynamics*,
511 pp.1-24.
512
513 Schneider, L., Smerdon, J.E., Büntgen, U., Wilson, R.J., Myglan, V.S., Kirilyanov, A.V. and Esper, J., 2015.
514 Revising midlatitude summer temperatures back to AD 600 based on a wood density network. *Geophysical*
515 *Research Letters*, 42(11), pp.4556-4562.
516
517 Schweingruber, F. 1988. *Tree Rings: Basics and Applications of Dendrochronology*. Springer, NY.
518
519 Solomina, O.N., Bradley, R.S., Jomelli, V., Geirsdottir, A., Kaufman, D.S., Koch, J., McKay, N.P., Masiokas, M.,
520 Miller, G., Nesje, A. and Nicolussi, K., 2016. Glacier fluctuations during the past 2000 years. *Quaternary Science*
521 *Reviews*, 149, pp.61-90.
522

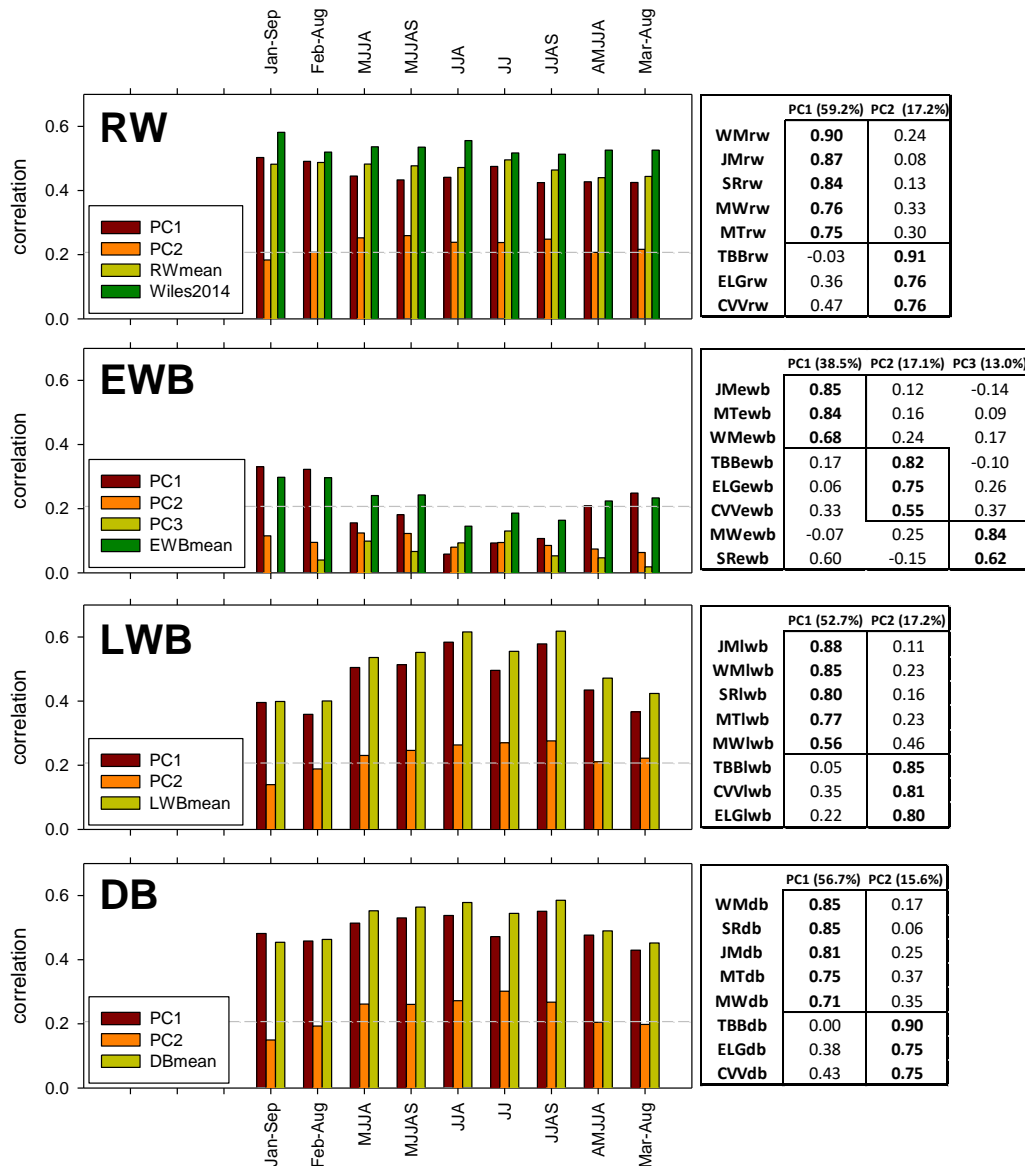


- 523 Wigley, T.M., Briffa, K.R. and Jones, P.D., 1984. On the average value of correlated time series, with applications
524 in dendroclimatology and hydrometeorology. *Journal of climate and Applied Meteorology*, 23(2), pp.201-213.
525
- 526 Wiles, G.C., D'Arrigo, R.D., Villalba, R., Calkin, P.E. and Barclay, D.J., 2004. Century-scale solar variability and
527 Alaskan temperature change over the past millennium. *Geophysical Research Letters*, 31(15).
528
- 529 Wiles, G.C., D'Arrigo, R.D., Barclay, D., Wilson, R.S., Jarvis, S.K., Vargo, L. and Frank, D., 2014. Surface air
530 temperature variability reconstructed with tree rings for the Gulf of Alaska over the past 1200 years. *The Holocene*,
531 24(2), pp.198-208.
532
- 533 Wilson, R.J. and Luckman, B.H., 2003. Dendroclimatic reconstruction of maximum summer temperatures from
534 upper treeline sites in Interior British Columbia, Canada. *The Holocene*, 13(6), pp.851-861.
535
- 536 Wilson, R., Rao, R., Rydval, M., Wood, C., Larsson, L.Å. and Luckman, B.H., 2014. Blue Intensity for
537 dendroclimatology: The BC blues: A case study from British Columbia, Canada. *The Holocene*, 24(11), pp.1428-
538 1438.
539
- 540 Wilson, R., K. Anchukaitis, K. Briffa, U. Büntgen, E. Cook, R. D' Arrigo, N. Davi, J. Esper, D. Frank, B.
541 Gunnarson, G. Hegerl, S. Klesse, P. Krusic, H. Linderholm, V. Myglan, Z. Peng, M. Rydval, L. Schneider, A.
542 Schurer, G. Wiles and E. Zorita. 2016. Last millennium northern hemisphere summer temperatures from tree rings:
543 Part I: The long term context. *Quaternary Science Reviews*, 134, pp.1-18.
544
- 545 Wilson, R., Wilson, D., Rydval, M., Crone, A., Büntgen, U., Clark, S., Ehmer, J., Forbes, E., Fuentes, M.,
546 Gunnarson, B.E. and Linderholm, H.W., 2017. Facilitating tree-ring dating of historic conifer timbers using Blue
547 Intensity. *Journal of Archaeological Science*, 78, pp.99-111.
548



549
550
551
552
553
554
555
556
557

Figure 1: Location map of the eight GOA tree-ring sites used in this study (Table 1). Also indicated (dashed line box) is the domain (57-61°N / 153-134°W) of the gridded data (CRU TS 3.24, Harris et al. 2012; BEST, Rohde et al., 2012) used for calibration and the five coastal GOA temperature stations used in the original 5-station mean series (Wilson et al. 2007 – see supplementary Figure 1).

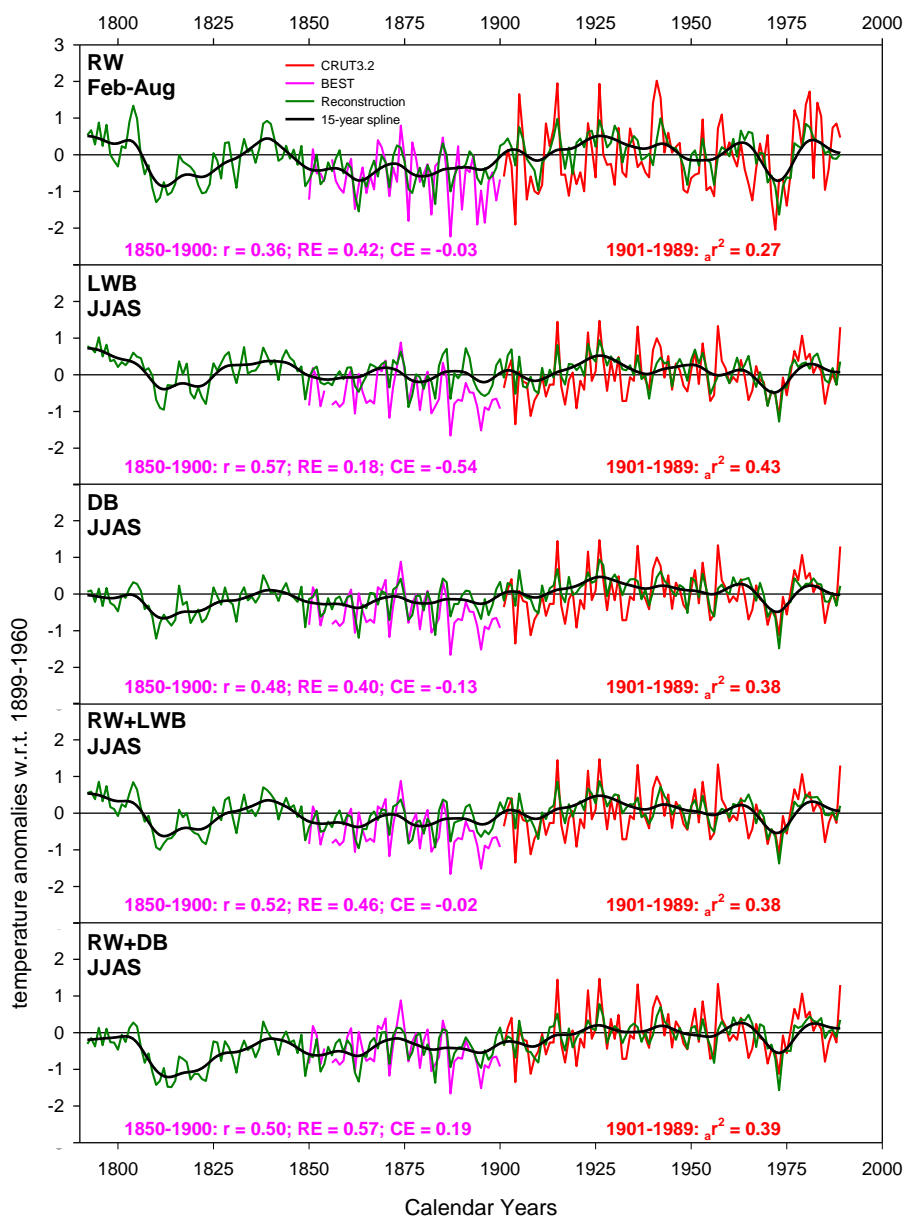


558
 559
 560
 561
 562
 563
 564
 565
 566
 567
 568

Figure 2: Left: Correlation response function analysis (1901-1989) using CRU TS3.24 mean temperatures with each tree-ring variable (RW = ring-width; EWB = early wood maximum blue intensity; LWB = inverted latewood minimum blue intensity; DB – Delta Blue). The bars represent correlations with seasonal temperature for each principal component (PC) score and the simple GOA mean composite. Also for RW, correlations are shown for the Wiles et al. (2014) RW based RCS reconstruction. Horizontal line denotes the 95% confidence limit. Correlations against individual months are presented in Supplementary Figure 2. **Right:** Varimax rotation principal component analysis results showing loadings of each chronology on each PC with an eigenvalue > 1.0. % values denote the explained amount of variance each PC explains of the original data input matrix.



569
 570
 571

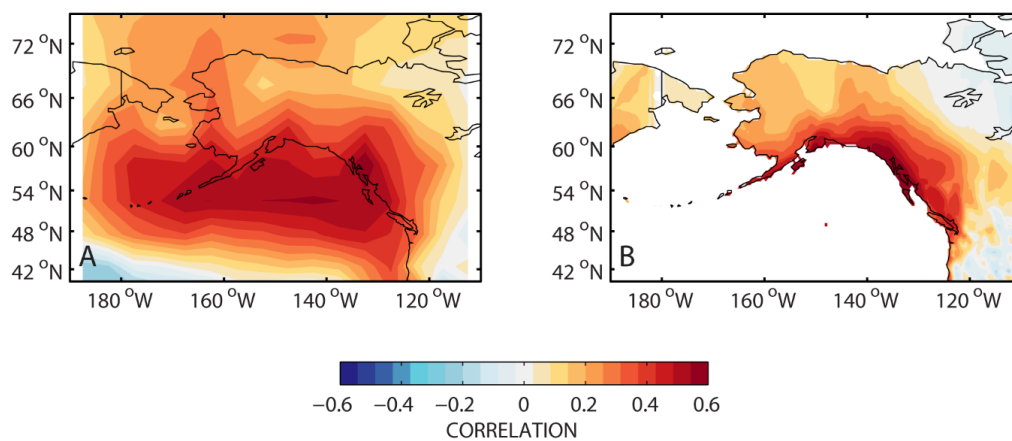


572
 573
 574
 575
 576
 577

Figure 3: Illustration of the various PC regression experiments performed herein, with each reconstruction model compared against the June-September (Table 3). Feb-August is shown for RW as that was the reconstructed season in Wiles et al. (2014). Full period calibration is performed on the 1901-1989 period (Table 3 – CRU TS 3.2.4) while validation (Pearson’s correlation coefficient (r), Reduction of Error (RE) and



578 Coefficient of Efficiency (CE)) is undertaken over 1850-1900 using the BEST gridded data after those data
579 were scaled to the CRU TS 3.24 data over the 1901-1989 period.
580
581

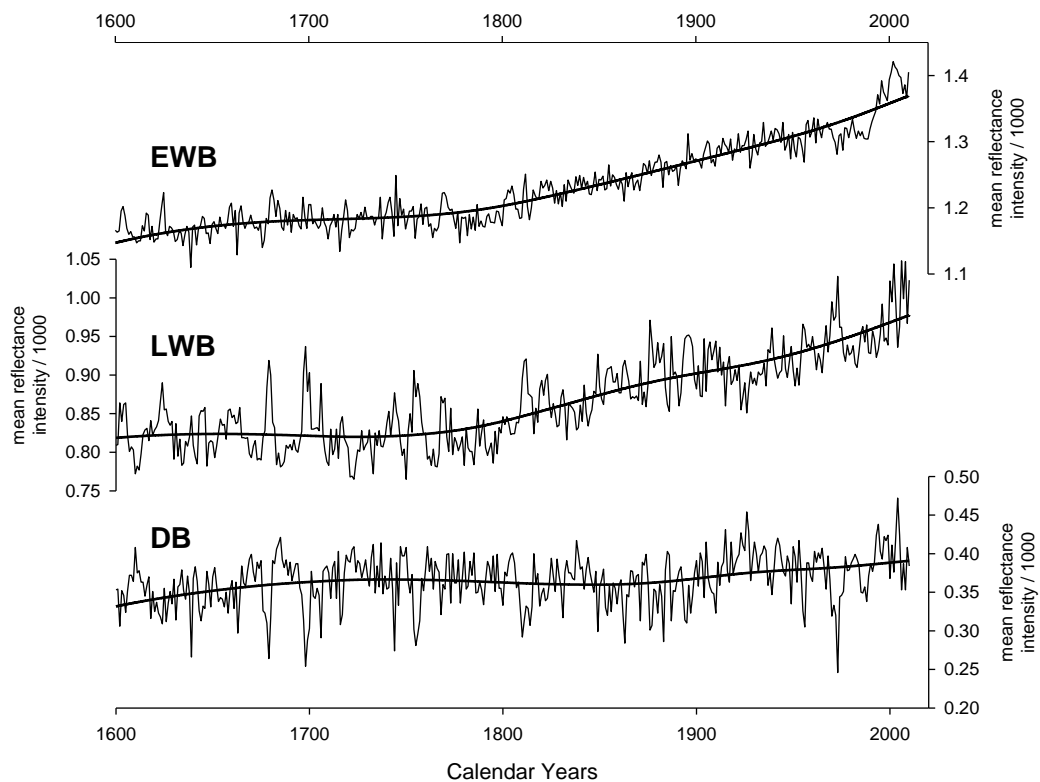


582

583 **Figure 4:** Spatial correlation (1901-1989) fields comparing the RW+DB GOA JJAS temperature reconstruction
584 with larger-scale temperatures. **A:** for HADCRUT4 land/SST (Morice et al. 2012; Cowtan and Way 2014); **B:**
585 for CRU TS3.24 land temperatures (Harris et al. 2012).

586

587



588

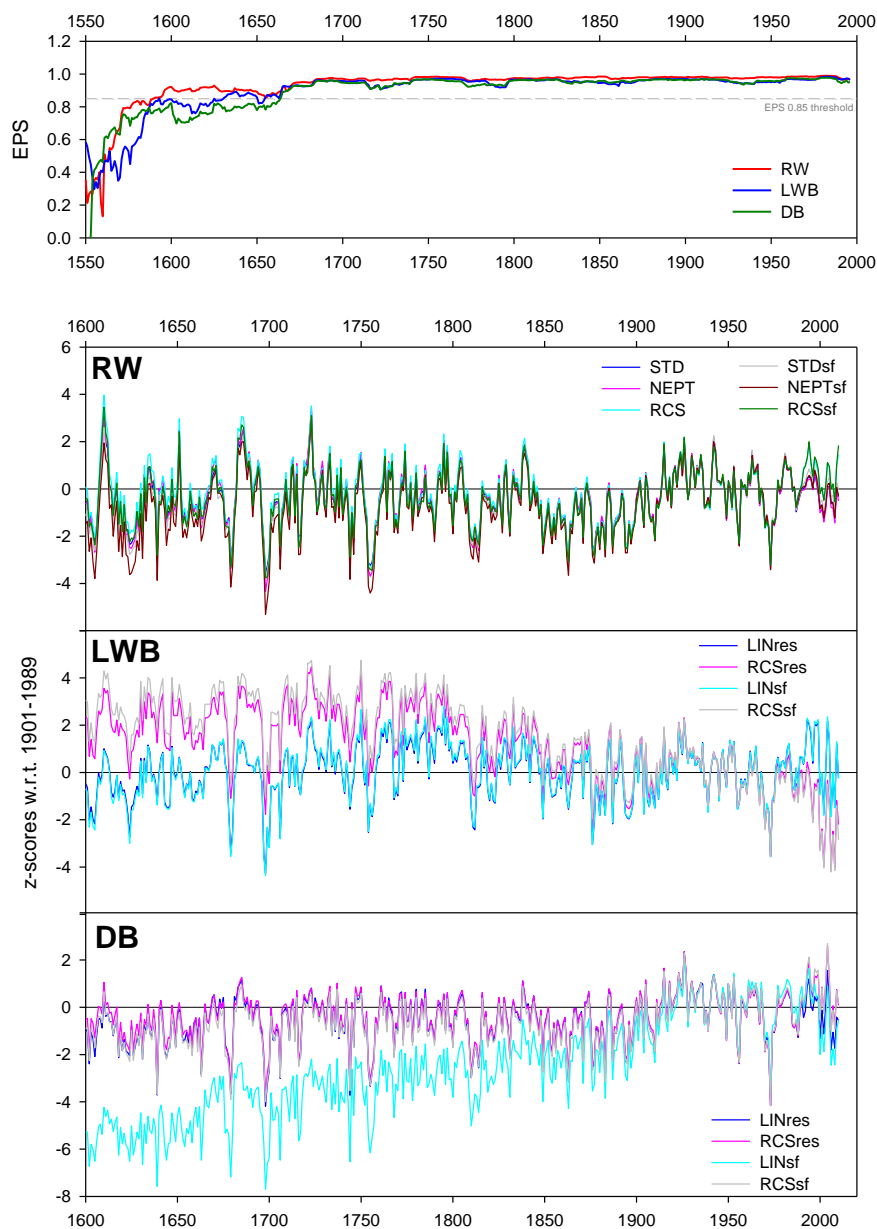
589

590

591

592

Figure 5: Mean non-detrended GOA wide composite chronologies since 1600 for EWB, LWB and DB. The LWB data have not been inverted for this figure.

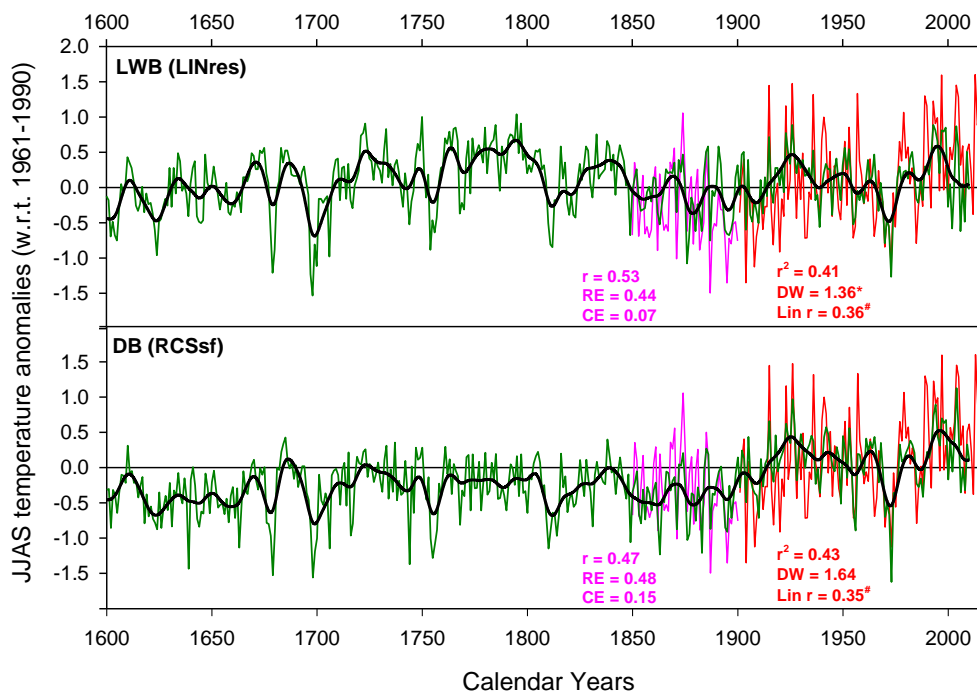


593
 594
 595
 596
 597
 598
 599
 600

Figure 6: Detrending experiments for each TR variable using the full GOA regional composite (data from all 8 sites). Upper panel is 31-year moving EPS plots for RW, LWB and DB using 200-yr spline detrending. Low plots present chronology variants from 1600-2010. For RW - STD = negative exponential detrending (ratio) or regression function of zero or negative slope; NEPT = as STD but raw data have been power transformed and detrended via subtraction; RCS = single group RCS detrending (ratio); STDsf, NEPTsf, RCSsf = as previous three options but using signal free detrending. For LWB and DB - LINres - detrending via subtraction using



601 linear functions (negative or zero slope); RCSres = as RCS above but detrending via subtraction; LINsf and
 602 RCSsf = as with LINres and RCSres but with signal free detrending.

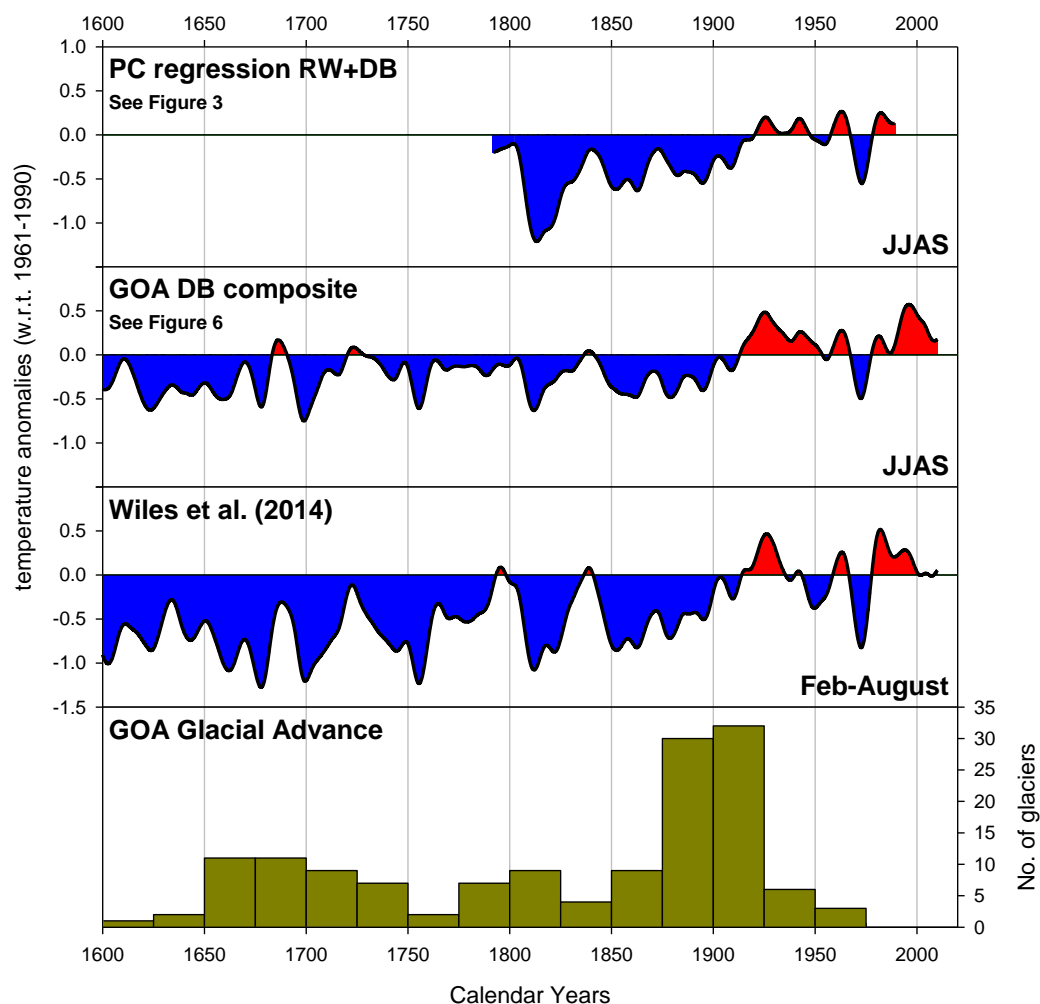


603

604

605 **Figure 7:** Extended reconstruction tests using LWB and DB. 1901-2010 period calibration uses CRU TS3.24
 606 data while validation is performed using BEST data over the 1850-1900 period. * denotes significant 1st order
 607 autocorrelation in model residuals; # denotes a significant linear trend in the model residuals.

608



609

610

611 **Figure 8:** Comparison of GOA reconstruction variants using DB and RW with Wiles et al. (2014). The lower
 612 panel presents a histogram of glacial advance in the GOA region (Wiles et al., 2004; Solomina et al. 2016).

613



Site Name	Timespan	No. of series	Period n > 5	MSL	RW RBAR	EWB RBAR	LWB RBAR	DB RBAR	N-RW EPS	N-EWB EPS	N-LWB EPS	N-DB EPS
Cordova Eyak Mtn (CVV)	1573-1992	17	1672-1992	280.6	0.46	0.15	0.32	0.29	6.5	32.1	12.0	14.2
Juneau Mtn (JM)	1558-1998	17	1604-1998	238.5	0.35	0.15	0.24	0.25	10.7	32.9	17.7	17.3
McGinnis (MT)	1485-1999	15	1584-1999	363.5	0.47	0.11	0.24	0.24	6.4	46.3	17.6	18.0
Miners Well (MW)	1479-1994	13	1640-1995	324.0	0.49	0.05	0.33	0.14	5.8	120.3	11.8	36.2
Son of Repeater (SR)	1713-2009	10	1792-2007	216.7	0.33	0.12	0.17	0.25	11.3	43.5	27.5	17.4
Wright Mtn (WM)	1610-2010	17	1738-2010	234.2	0.45	0.06	0.25	0.17	6.9	84.0	17.1	27.9
Ellsworth (ELG)	1636-1991	18	1750-1990	218.5	0.40	0.14	0.24	0.29	8.6	35.7	17.7	14.2
Tebenkof (TBB)	1357-1990	15	1605-1990	339.2	0.43	0.13	0.20	0.22	7.6	37.9	22.4	19.6
			median	259.6	0.44	0.12	0.24	0.24	7.2	40.7	17.6	17.7

Table 1: Metadata information for the eight GOA sites used in the study. All PCA and related analyses were performed on the 1792-1990 period for which there is replication for all eight sites of at least five series. Tree-ring data were detrended using a 200-year spline for these signal strength analyses. The final 4 columns denote the number of series needed to attain an EPS of 0.85 (Wigley et al. 1984).

RW									
	JM	MT	SR	WM	MW	CVV	TBB	ELG	
1850-1900	0.45	0.22	0.49	0.22	0.27	0.30	0.30	0.38	
1901-1990	0.49	0.26	0.42	0.41	0.36	0.41	0.20	0.34	
1850-1990	0.50	0.37	0.47	0.43	0.39	0.47	0.33	0.39	
LWB									
	JM	MT	SR	WM	MW	CVV	TBB	ELG	
1850-1900	0.45	0.29	0.48	0.38	0.49	0.40	0.25	0.46	
1901-1990	0.52	0.39	0.64	0.58	0.46	0.45	0.28	0.41	
1850-1990	0.37	0.32	0.55	0.46	0.53	0.51	0.33	0.44	
DB									
	JM	MT	SR	WM	MW	CVV	TBB	ELG	
1850-1900	0.45	0.29	0.49	0.23	0.35	0.40	0.37	0.48	
1901-1990	0.57	0.45	0.58	0.47	0.48	0.50	0.23	0.39	
1850-1990	0.53	0.44	0.48	0.38	0.44	0.52	0.34	0.44	

Table 2: Correlations (1850-1900, 1901-1990 and 1850-1990) for each site RW, LWB and DB chronology against JJAS temperatures. EWB correlations are not shown. The sites are ordered from east to west (see Figure 1).

mean r	EWB	LWB	DB
RW	0.27	0.68	0.81
EWB		-0.23	0.36
LWB			0.80

Table 3: Correlation matrix between the different tree-ring variable chronologies (200-year spline detrended). These values represent the averages for between TR variable correlations performed separately for each site.

614
615
616
617
618
619
620
621

622
623
624
625
626
627
628

629
630
631
632
633
634



Wiles14	season	1901-1960 Calibration			1961-1989 Validation			1901-1989 Full Calibration + Residuals			
		series entered	r	r2	r	RE	CE	r	r2	DW	Linr
	MJJA	Wiles2014	0.60	0.36	0.48	0.11	0.10	0.55	0.30	1.62	0.15
	MJJAS	Wiles2014	0.55	0.30	0.53	0.21	0.20	0.53	0.28	1.72	0.17
	JJA	Wiles2014	0.58	0.34	0.47	0.06	0.05	0.53	0.28	1.75	0.17
	JJAS	Wiles2014	0.52	0.27	0.53	0.20	0.20	0.51	0.26	1.77	0.18
	Feb-Aug	Wiles2014	0.60	0.36	0.54	0.23	0.23	0.57	0.33	1.78	0.17
RW	season	PCs entered	r	ar2	r	RE	CE	r	ar2	DW	Linr
	MJJA	1, 2	0.60	0.34	0.40	0.03	0.03	0.52	0.26	1.60	0.21
	MJJAS	1, 2	0.56	0.29	0.46	0.15	0.14	0.52	0.25	1.70	0.23
	JJA	1, 2	0.58	0.31	0.42	-0.01	-0.02	0.51	0.24	1.74	0.23
	JJAS	2, 1	0.53	0.26	0.49	0.16	0.15	0.51	0.24	1.76	0.24
	Feb-Aug	2, 1	0.60	0.36	0.46	0.08	0.08	0.54	0.27	1.75	0.23
LWB	season	PCs entered	r	ar2	r	RE	CE	r	ar2	DW	Linr
	MJJA	1, 2	0.63	0.38	0.49	0.15	0.14	0.57	0.31	1.39	0.20
	MJJAS	1, 2	0.63	0.37	0.55	0.23	0.22	0.59	0.34	1.50	0.23
	JJA	1, 2	0.71	0.49	0.58	0.16	0.15	0.66	0.42	1.45	0.25
	JJAS	1, 2	0.69	0.46	0.64	0.27	0.27	0.66	0.43	1.51	0.27
DB	season	PCs entered	r	ar2	r	RE	CE	r	ar2	DW	Linr
	MJJA	1, 2	0.69	0.45	0.43	-0.01	-0.02	0.59	0.33	1.55	0.24
	MJJAS	1, 2	0.67	0.43	0.50	0.09	0.08	0.61	0.37	1.68	0.26
	JJA	1, 2	0.70	0.47	0.50	-0.05	-0.05	0.62	0.36	1.65	0.26
	JJAS	1, 2	0.68	0.44	0.58	0.11	0.11	0.63	0.38	1.72	0.29
RW + LWB	season	PCs entered	r	ar2	r	RE	CE	r	ar2	DW	Linr
	MJJA	1, 2	0.69	0.45	0.46	0.03	0.03	0.60	0.34	1.67	0.18
	MJJAS	1, 2	0.66	0.43	0.51	0.13	0.12	0.62	0.37	1.87	0.20
	JJA	1, 2, 3	0.72	0.49	0.52	-0.07	-0.08	0.63	0.37	1.56	0.26
	JJAS	1, 2, 3	0.68	0.43	0.59	0.12	0.12	0.63	0.38	1.63	0.28
RW + DB	season	PCs entered	r	ar2	r	RE	CE	r	ar2	DW	Linr
	MJJA	1, 2	0.71	0.49	0.44	-0.16	-0.16	0.62	0.36	1.69	0.04
	MJJAS	1, 2	0.72	0.51	0.49	-0.14	-0.15	0.61	0.36	1.78	-0.11
	JJA	1, 2, 3	0.72	0.50	0.49	-0.15	-0.15	0.56	0.32	1.89	-0.12
	JJAS	1, 2	0.71	0.49	0.52	-0.18	-0.18	0.64	0.39	1.84	0.05

635
636
637
638
639
640
641
642
643

Table 4: Calibration experiments for four dominant seasons (see Figure 2). Initial calibration (using CRU TS 3.24) was made over 1901-1960 and validation over 1961-1989. Full calibration (1901-1989) was also performed to allow for residual tests and extra validation using BEST (1850-1990 – see Figure 2). Shaded results do not pass significance. r = Pearson's correlation coefficient; r2 = coefficient of determination; ar2 = r2 adjusted for the number of predictors in the model; RE = Reduction of Error; CE = Coefficient of Efficiency; DW = Durbin-Watson test for residual autocorrelation; LINr = linear trend of the residuals.



	1901-2010 Calibration					1850-1900 Validation		
	series entered	r	r2	DW	LINr	r	RE	CE
LWB	LINres	0.64	0.41	1.36	0.36	0.53	0.44	0.07
	RCSres	0.26	0.07	1.28	0.48	0.56	0.01	-0.64
	LINsf	0.64	0.41	1.37	0.36	0.53	0.43	0.06
	RCSsf	0.21	0.05	1.32	0.46	0.56	-0.05	-0.73
	1901-2010 Calibration					1850-1900 Validation		
	series entered	r	r2	DW	LINr	r	RE	CE
DB	LINres	0.55	0.31	1.37	0.50	0.50	0.52	0.21
	RCSres	0.64	0.40	1.59	0.40	0.48	0.50	0.18
	LINSF	0.54	0.29	1.35	0.38	0.43	0.40	0.00
	RCSsf	0.65	0.43	1.64	0.35	0.47	0.48	0.15

644

645

646

647

Table 5: Extended reconstruction Calibration experiments using different chronology versions (Figure 6) of LWB and DB. Shaded results do not pass significance.